Nanomaterials

DOI: 10.1002/ange.201301069

Improving Hydrothermal Carbonization by Using Poly(ionic liquid)s**

Pengfei Zhang, Jiayin Yuan, Tim-Patrick Fellinger, Markus Antonietti, Haoran Li, and Yong Wang**

Functional carbonaceous materials with high specific surface areas and controllable structural compositions have been an appealing topic in recent years, owing to their wide applications in various fields.[1] So far, a number of well-known synthetic methods including thermal pyrolysis of organic compounds,[2a] high-voltage-arc electricity,[2b] laser ablation,[2c] and chemical vapor deposition,[2d] have been developed for the preparation of carbon materials with different sizes, shapes, and chemical compositions. Nowadays, energy and sustainability issues are seriously considered when designing synthetic strategies. The recently rediscovered environmentally friendly and facile hydrothermal carbonization (HTC) procedure offers new perspectives, as it involves the use of renewable resources (e.g., cellulose) at low temperatures (130–250 °C) in aqueous medium under self-generated pressure.[3] Materials prepared by this straightforward water-based method are commonly nonporous and have unfavorably low surface areas ($< 20\ m^2 g^{-1}$).[3a] To induce pore formation, both hard- and soft-templating strategies, and some other efficient techniques (such as the use of metal salts or protein additives) have been recently introduced into the HTC process.[4] For example, a novel borax-mediated HTC method was reported to produce aerogel materials that have similarities to the traditional resorcinol–formaldehyde-based organic aerogels.[4i] Considering practical applications, HTC carbonaceous materials with not only porous nanostructures but also more specific features (e.g., heteroatom or metal nanoparticle doping) are highly desirable and of great potential, in particular for catalysis.

Herein, we report an improvement of HTC through template-free poly(ionic liquid)s (PILs) assisted structure formation, a facile yet efficient process to prepare nanostructured porous nitrogen-doped carbon materials (S_{BET} up to $572\ m^2 g^{-1}$) from inexpensive, harmless, and naturally available sugars by HTC at 160–200 °C, followed by a post-synthesis heating treatment. PILs are surface-active and multifunctional polyelectrolytes made up of ionic liquid (IL) repeating units joined in a polymer chain.[5] Although the originally designed role of PILs here was only to effectively stabilize the primary carbon nanoparticles formed by HTC, their unexpectedly versatile properties were quickly recognized and enabled the formation of more diverse products. For example, this approach was successfully coupled with metal salts to directly produce novel porous nanohybrids (S_{BET} up to $255\ m^2 g^{-1}$) of Au–Pd core-shell nanoparticles trapped in N-doped carbon materials, which served as active and highly recyclable (reused forty times) catalysts for the selective semihydrogenation of phenylacetylene under mild reaction conditions (80 °C, H_2 1 atm).

HTC of D-fructose and D-glucose was performed at 160–200 °C in the presence of different ILs and PILs (Figure 1). The products are denoted as Fru-PILa-1.2@160, etc., where

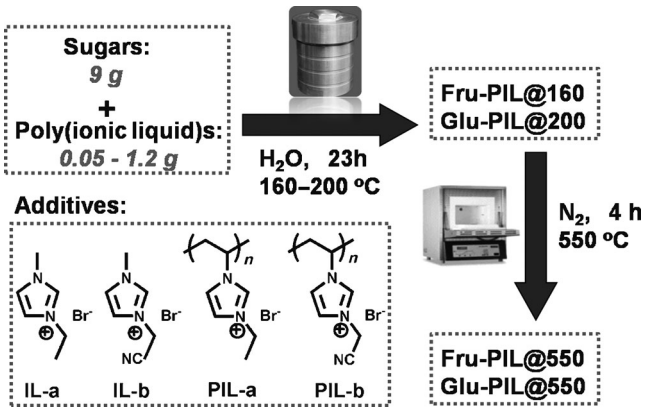

Figure 1. Synthetic route to porous nitrogen-doped carbon nanostructures by a HTC-PILs protocol.

PILa-1.2 corresponds to the type and amount (g) of additive per 9 g of sugar and the last number, in this case 160, denotes the carbonization temperature. Figure 2, Figure S1, and Figure S2 show the scanning-electron-microscopy (SEM) micrographs of several HTC carbon materials. The HTC carbon materials obtained from pure fructose are micrometer sized, spherical particles (diameter: 2.3 ± 0.5 μm; Figure 2a). When 0.1–1.2 g of PILb additive is used, the particle size drops

[*] P. F. Zhang, Prof. Dr. H. R. Li, Prof. Dr. Y. Wang
ZJU-NHU United R&D Center
Key Lab of Applied Chemistry of Zhejiang Province
Department of Chemistry
Zhejiang University
Hangzhou 310028 (P. R. China)
E-mail: chemwy@zju.edu.cn
Homepage: http://mypage.zju.edu.cn/chemwy
Dr. J. Yuan, Dr. T.-P. Fellinger, Prof.Dr. M. Antonietti
Abteilung Kolloidchemie
Max-Planck-Institut für Kolloid- und Grenzflächenforschung
Golm, Potsdam 14424 (Germany)
E-mail: Jiayin.Yuan@mpikg.mpg.de

[**] Financial support from the Joint Petroleum and Petrochemical Funds of the National Natural Science Foundation of China and China National Petroleum Corporation (U1162124), Specialized Research Fund for the Doctoral Program of Higher Education (J20130060), the Fundamental Research Funds for the Central Universities, the Program for Zhejiang Leading Team of S&T Innovation, and the Partner Group Program of the Zhejiang University and the Max-Planck Society are greatly appreciated.

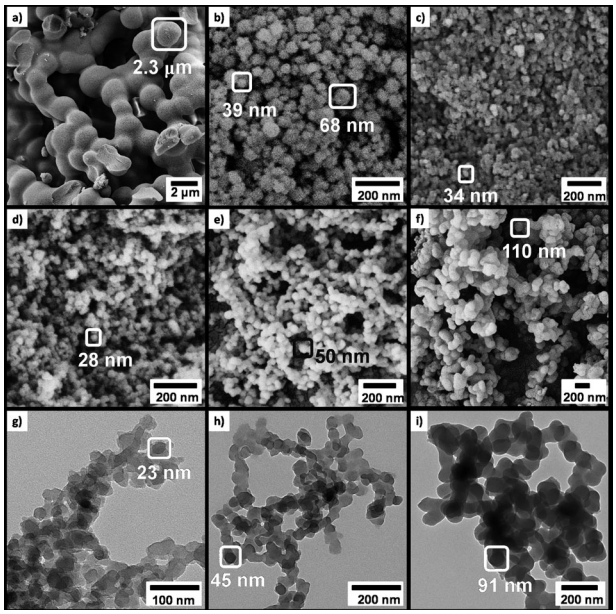

Figure 2. SEM images of carbon materials: a) Fru@160; b) Fru-PILb-1.2@160; c) Fru-PILb-0.6@160; d) Fru-PILb-0.3@160; e) Fru-PILb-0.1@160; f) Fru-PILb-0.05@160. TEM images of HTC carbon materials: g) Fru-PILb-0.3@160; h) Fru-PILb-0.1@160; i) Fru-PILb-0.05@160

Table 1: Yield, specific surface area, and elemental composition of the as-prepared carbon materials.

Carbon Material	Yield [g][a]	S_{BET} [$m^2 g^{-1}$][b]	Pore Size [nm]	Pore Volume [$cm^3 g^{-1}$]	N [%][c]
Fru@160	27	<10	1.7	0.01	–
Glu@200	38	<10	1.5	0.01	–
Fru-ILa-1.2@160	25	<10	1.9	0.02	0.5
Fru-ILb-1.2@160	43	<5	1.8	0.01	1.7
Fru-PILa-1.2@160	70	37	1.5	0.19	2.3
Fru-PILb-1.2@160	65	129	2.2	0.30	4.8
Fru-PILb-0.6@160	48	161	7.1	0.32	2.4
Fru-PILb-0.3@160	57	134	10.8	0.34	1.4
Fru-PILb-0.1@160	36	81	8.8	0.15	–
Fru-PILb-0.05@160	43	26	10	0.04	–
Glu-PILb-0.3@160	36	160	9.7	0.43	1.5
Fru@550	11	82	1.7	<0.01	–
Fru-PILa-1.2@550	31	315	1.7	0.14	2.1
Fru-PILb-1.2@550	31	181	1.9	0.21	4.6
Fru-PILb-0.6@550	28	464	5.9	0.27	2.7
Fru-PILb-0.3@550	31	476	6.0	0.24	1.6
Fru-PILb-0.1@550	20	572	8.6	0.35	–
Fru-PILb-0.05@550	22	481	4.7	0.08	–
Glu-PILb-0.3@550	20	496	8.1	0.37	1.7

[a] Yield per 100 grams of sugar. [b] Specific surface area calculated using the BET method for the adsorption data in the relative pressure interval from 0.05 to 0.35. [c] Nitrogen content obtained from elemental analysis.

considerably and can be finely restricted in the range of 20–50 nm (Figure 2b–e). At an even lower loading (0.05 g) of PILb, the formed particles are approximately 110 nm in diameter, which is still significantly smaller than those obtained from reactions in the absence of PILs (Figure 2f). The TEM images (Figure 2g–i) indicate that these carbon nanospherules form a hierarchical porous aggregation network, favorable for heterogeneous catalysis.[6]

A general HTC procedure involves dehydration of fructose to 5-hydroxymethyl furfural, followed by condensation/polymerization reactions. The resulting polyfuran-type units precipitate, once supersaturated, from the homogeneous solution, and then aggregate into secondary spherical particles of the final size.[7] The role of PILs as a universal stabilizer for many systems has been confirmed in previous literature.[5a] Here, the PILs chains stabilize the primary nanoparticles formed at the initial stage and allow only growth by further addition of monomers. The charge of the PILs introduces electrostatic repulsion to keep the nanoparticles stable in solution and minimize their agglomeration, thus efficiently lowering the primary particle size from 2.3 µm down to <50 nm. At later stages of the reaction, the overall concentration of those small primary entities becomes so high that they intergrow to form the final hierarchical network, as also known from silica and resorcinol–formaldehyde resins.[8]

The pore structure of the HTC products was examined by nitrogen sorption measurements (Table 1). The carbon products derived from pure sugars or with IL additives showed small surface areas ($S_{BET}<10\ m^2 g^{-1}$; Figure S3). This finding is in agreement with previous work on the unmodified HTC of glucose.[3a] In comparison, the use of PIL additives, at weight fractions of 0.55–13.3%, significantly increased specific surface areas (Figure 3 and Figure S4). Among these

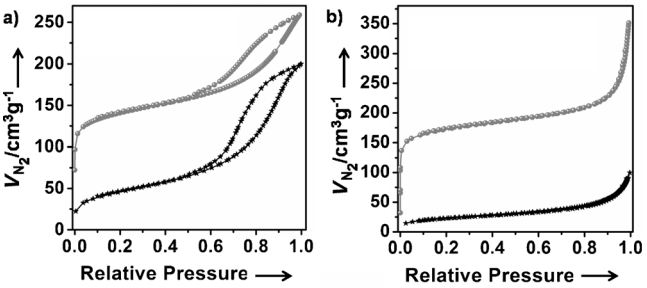

Figure 3. Nitrogen sorption isotherms for the carbon materials. a) Fru-PILb-0.6@160 (black); Fru-PILb-0.6@550(gray). b)a) Fru-PILb-0.1@160 (black); Fru-PILb-0.1@550(gray).

HTC materials, Fru-PILb-0.6@160 had the highest specific surface area ($161\ m^2 g^{-1}$), and presented type IV hysteresis characteristics of mesoporous materials with a condensation step around $p/p_0 \approx 0.6$ (Figure 3a). The better performance of PILs over ILs in the formation of pores is assigned to the multivalent binding power of PILs. The post-synthesis carbonization at moderate temperature (550°C) further improved the textural properties as a result of the strong micropore evolution, thus increasing the S_{BET} value up to $572\ m^2 g^{-1}$ (Figure 3b). As an abundant sugar type, glucose could also be smoothly transformed into porous carbon materials ($S_{BET}=496\ m^2 g^{-1}$) with the use of 3.3 wt% of PILb additive. The yield of the HTC of pure fructose (Fru@160: 27%) was lower than those of HTC with PILs additives (36–70%; Table 1), another proof of the catalytic effect of PILs in accelerating the HTC of sugars. Thus the aforementioned results nicely demonstrate the benefit of PILs additives to

control the yield and porosity (micropore and mesopore) in HTC; this control is inaccessible when using only thermal treatment.[3d]

The introduction of PILs, especially PILb with a nitrile group, simultaneously incorporated nitrogen into the products. The amount of nitrogen is up to approximately 4.8 wt% in the carbon materials when 13.3 wt% of PILb additive is used (Table 1). This result means that practically all the PILs ends up in the product. When further carbonized at 550°C, the nitrogen content stayed constant, thus suggesting that most of the nitrogen is incorporated into the carbon matrix upon HTC. X-ray photoelectron spectroscopy (XPS) analysis revealed that the N1s region contained an intense quaternary-type motif (401.6 eV; 91.5%), which might be produced in the condensation of a nitrile group, and some pyridinic nitrogen atoms (398.7 eV: 8.5%; Figure S5). These results prove the role of PILs as a nitrogen source in the formation of the nanostructures; the inclusion of nitrogen atoms into the carbon materials might modify some of their properties, for example, electrical conductivity, basicity, oxidation stability, and catalytic activity.[9] X-ray diffraction (XRD) patterns of the original HTC carbon materials presented a broad peak around 20°, in agreement with their amorphous state and more resin-like character (Figure S6).

Next, we wanted to illustrate the flexibility of the HTC–PILs protocol by a direct synthesis of porous Au–Pd@N-carbon nanohybrids, where fructose serves both as carbon source and reducing agent, and $PdCl_2$ and $HAuCl_4$ as metal sources, because previous work indicated these HTC carbon materials held remarkable capability for in situ loading of metal nanoparticles.[10a–b] Four Au–Pd@N-Carbon materials with different metal loadings were obtained as dark brown powders with good yields (Figure S7). These materials were denoted as 2.1%Au–2.5%Pd@N-Carbon, etc., in which the 2.1% and 2.5% correspond to the metal content.

XRD patterns of the products confirmed the existence of Au^0, Pd^0, and PdO in the materials (Figure S8). The peaks in 2.1%Au–2.5%Pd@N-Carbon can be indexed as (111), (200), and (220) diffraction planes of metallic Au, (111) plane reflection of Pd particles, and (101) plane of PdO. The average size of the Au–Pd crystallite was calculated, by using Scherrer's formula, to be approximately 27 nm from the Pd (111) peak, which is larger than the size (ca. 12 nm) calculated from the Au (111) peak. The Au–Pd@N-Carbon hybrids after HTC at 160°C exhibited type IV/H_3 sorption isotherms with S_{BET} values up to 255 $m^2 g^{-1}$, which to the best of our knowledge are the highest values among those of various metal/carbon composites prepared in a single step by HTC (Figure S9, Table 2).[10] As expected, all these materials were doped with approximately 5 wt% of nitrogen, as determined by elemental analysis.

TEM images of Au–Pd@N-Carbon show that these nanosized metallic particles are well dispersed on the carbon support (Figure S10). A particle composed of both Au and Pd was confirmed by STEM-EDX analysis (Figure S11). Au–Pd core-shell nanoparticles with a Au core and a Pd shell have recently been shown to have enhanced properties relative to their monometallic counterparts in many fields.[11] A detailed HRTEM analysis of a number of these alloy crystals suggests

Table 2: Characterization of Au–Pd@N-Carbon and its application in the hydrogenation of phenylacetylene.[a]

Sample	S_{BET} [$m^2 g^{-1}$][b]	N [%][c]	*t* [min]	Conv. [%]	Selectivity [%][d] =C	−C
–	–		240	<1	–	–
2.5%Pd@N-Carbon	118	5.9	60	96	88	9
2.1%Au@N-Carbon	95	5.1	240	12	92	4
2.1%Au-2.5%Pd @N-Carbon	255	6.3	40	94	85	10
0.95%Au-1.1%Pd @N-Carbon	85	5.5	70	99	89	8

[a] Reaction conditions: phenylacetylene (1 mmol), catalyst (50 mg), decane (110 μL; internal standard), ethanol (10 mL), H_2 balloon (1 atm), 80°C. [b] Specific surface area calculated using the BET method. [c] Nitrogen content obtained from elemental analysis. [d] Selectivity for styrene (=C) and ethylbenzene (−C).

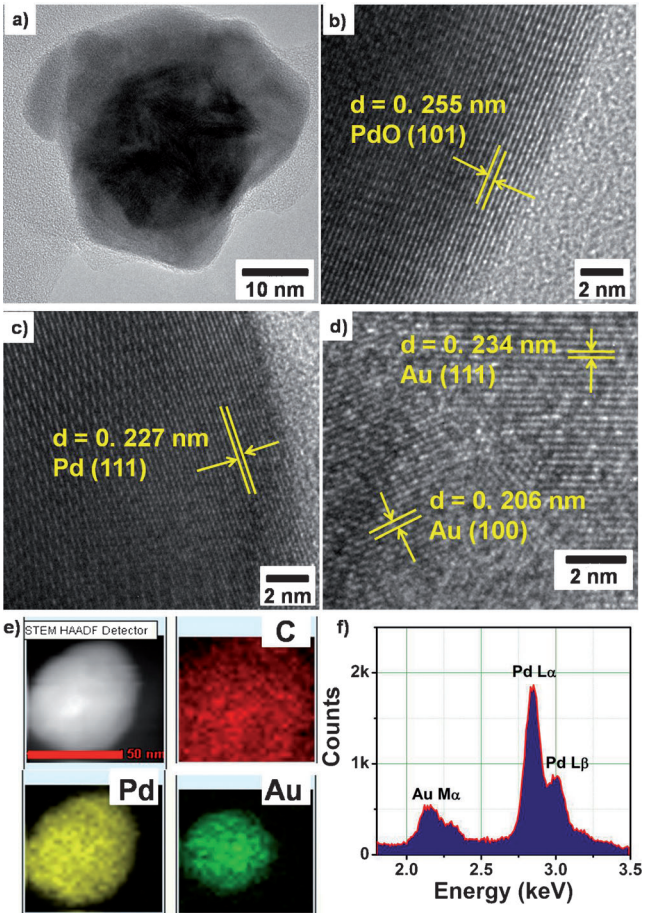

Figure 4. a)–d) HRTEM images of a representative Au–Pd particle embedded in 0.95%Au–1.1%Pd@N-Carbon. e) A representative STEM-HAADF image of a Au–Pd particle in 0.95%Au–1.1%Pd@N-Carbon, and the corresponding STEM-XEDX maps of the C-Kα, Pd-Lα, and Au-Lα signals. Scale bar: 50 nm. f) The corresponding STEM-EDX point spectra.

that the Au–Pd particles embedded in the porous carbon material seem to adopt a core-shell configuration (Figure 4). The lattice spacings at the edge of Au–Pd particle were measured to be 0.255 nm and 0.227 nm, which are in good

agreement with that of crystalline PdO and metallic Pd, respectively (Figure 4b and c). Yet lattice planes assigned to the (100) and (111) facets of metallic Au can be observed only in the interior part (Figure 4d). To verify the structural and compositional details of Au–Pd particle, scanning electron transmission microscopy in high angular dark field mode (STEM-HAADF) and scanning electron transmission microscopy–X-ray energy dispersive spectroscopy (STEM-XEDS) mapping analysis was carried out for a representative spherical Au–Pd particle (Figure 4e and f). The Pd X-ray signal completely covers the spatial area of the Au–Pd STEM-HAADF image; however, the Au X-ray signal only originates from the inner circular region, in agreement with the XRD analysis that in the Au–Pd alloy, the Au crystallite is smaller than the Pd particle, thus giving straightforward evidence for the core-shell structure of supported Au–Pd nanoparticles, with a Pd-rich shell surrounding a spherical Au-rich core.

The selective semihydrogenation of phenylacetylene to styrene is an important industrial reaction to remove phenylacetylene residue from styrene. In spite of the development of a number of catalysts (both homogeneous and heterogeneous catalysts) that promote this selective hydrogenation,[12] an ideal catalyst, which is active, selective, recyclable, and works under mild conditions, is still eagerly pursued. The Au–Pd@N-Carbon hybrids were tested in this reaction under comparably mild conditions (80 °C, H_2 1 atm). When 2.5 % Pd@N-Carbon was used, 96 % phenylacetylene conversion was reached in 60 min, with good selectivity for styrene (Table 2). Interestingly, the 2.1 % Au–2.5 % Pd@N-Carbon was more active, giving 94 % conversion in 40 min, although the 2.1 % Au@N-Carbon was inactive in this process. It reveals that the Au–Pd core-shell configuration showed a positive influence on the catalytic properties. We hypothesize that the Au core may act as an electronic promoter for the Pd shell, which is beneficial for Pd-mediated hydrogenation.[11b] The reaction catalyzed by 0.95 % Au–1.1 % Pd@N-Carbon and thereby with lower metal content, still afforded 99 % phenylacetylene conversion in 70 min with 89 % selectivity towards styrene.

As a heterogeneous catalyst, the Au–Pd@N-Carbon system can be easily separated by centrifugation and washing with ethanol for recyclability tests. The 0.95 % Au–1.1 % Pd@N-Carbon could be reused at least forty times without significant loss of activity (Figure 5 and Table S1). The activity of the recovered catalyst was fully retained in the first thirty runs. From the 31st to 40th run, a longer reaction time was needed to keep the phenylacetylene conversion above 80 %. The gradually decrease in activity can be attributed to the loss of catalyst in the recovery process, as only 46 wt % of catalyst was recovered after forty runs. The average recovery ratio per run (ca. 98 wt %) is still satisfactory. The metal content of the recovered catalyst was investigated by ICP–AES, and the calculated leaching rate per run is rather low (< 1 %).

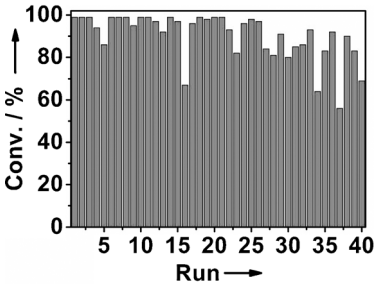

Figure 5. The reusing tests of 0.95 %Au–1.1 %Pd@N-Carbon in the phenylacetylene hydrogenation.

In summary, we demonstrated the use of PILs to improve the hydrothermal carbonization of ordinary sugars in terms of the structure, property, and function of the carbon products, which are porous, nitrogen-containing, and composed of primary spherical nanoparticles. PILs were believed to have many different roles in this process, that is, as stabilizer, pore-generating agent, and nitrogen source. The HTC carbon materials could be further modified by a post-synthesis carbonization step to amplify their porosity. This HTC–PILs strategy was extended to the one-step fabrication of Au–Pd core-shell nanoparticles supported by porous N-doped carbon materials. They were successfully applied as effective and easy-to-recycle catalysts in the selective hydrogenation of phenylacetylene under mild conditions. We believe that the current PILs-based HTC process to control structure and composition can be further optimized in terms of the anion type and PILs macromolecular architecture, to afford a set of functional carbon materials (with other incorporated heteroatoms) or metal/carbon hybrids by HTC.

Received: February 6, 2013
Published online: April 16, 2013

Keywords: hydrothermal synthesis · nanostructures · nitrogen doping · poly(ionic liquid)s · porous materials

[1] a) J. Lee, J. Kim, T. Hyeon, *Adv. Mater.* **2006**, *18*, 2073 – 2094; b) M. Sevilla, A. B. Fuertes, *Energy Environ. Sci.* **2011**, *4*, 1765 – 1771; c) Y. Wang, J. Zhang, X. Wang, M. Antonietti, H. Li, *Angew. Chem.* **2010**, *122*, 3428 – 3431; *Angew. Chem. Int. Ed.* **2010**, *49*, 3356 – 3359; d) B. Guo, M. Chi, X. G. Sun, S. Dai, *J. Power Sources* **2012**, *205*, 495 – 499; e) X. Wang, H. Zhu, F. Yang, X. Yang, *Adv. Mater.* **2011**, *23*, 2745 – 2748; f) K. P. Gong, F. Du, Z. H. Xia, M. Durstock, L. M. Dai, *Science* **2009**, *323*, 760 – 764; g) K. Nakanishi, N. Tanaka, *Acc. Chem. Res.* **2007**, *40*, 863 – 873.

[2] a) J. Lee, X. Wang, H. Luo, S. Dai, *Adv. Mater.* **2010**, *22*, 1004 – 1007; b) R. Lee, P. Nikolaev, H. Dai, P. Petit, C. Xu, Y. H. Lee, S. G. Kim, D. Colbert, G. Scuseria, D. Tománek, R. Smalley, *Science* **1996**, *273*, 483 – 487; c) T. Guo, P. Nikolaev, A. Rinzler, D. TomBnek, D. Colbert, R. Smalley, *J. Phys. Chem.* **1995**, *99*, 10694 – 10697; d) A. Eftekhari, P. Jafarkhani, F. Moztarzadeh, *Carbon* **2006**, *44*, 1343 – 1345.

[3] a) B. Hu, K. Wang, L. Wu, S. H. Yu, M. Antonietti, M. M. Titirici, *Adv. Mater.* **2010**, *22*, 813 – 828; b) X. L. Li, T. J. Lou, X. M. Sun, Y. D. Li, *Inorg. Chem.* **2004**, *43*, 5442 – 5449; c) Y. Fang, D. Gu, Y. Zou, Z. Wu, F. Li, R. Che, Y. Deng, B. Tu, D. Y. Zhao, *Angew. Chem.* **2010**, *122*, 8159 – 8163; *Angew. Chem. Int. Ed.* **2010**, *49*, 7987 – 7991; d) L. Yu, C. Falco, J. Weber, R. White, J. Howe, M. M. Titirici, *Langmuir* **2012**, *28*, 12373 – 12383; e) M. Sevilla, A. B. Fuertes, *Carbon* **2009**, *47*, 2281 – 2289.

[4] a) S. Jun, S. H. Joo, R. Ryoo, M. Kruk, M. Jaroniec, Z. Liu, T. Ohsuna, O. Terasaki, *J. Am. Chem. Soc.* **2000**, *122*, 10712 – 10713; b) C. Liang, S. Dai, *J. Am. Chem. Soc.* **2006**, *128*, 5316 – 5317; c) F. Zhang, Y. Meng, D. Gu, Y. Yan, C. Yu, B. Tu, D. Y. Zhao, *J.*

Am. Chem. Soc. **2005**, *127*, 13508 – 13509; d) A. H. Lu, B. Spliethoff, F. Schüth, *Chem. Mater.* **2008**, *20*, 5314 – 5319; e) M. M. Titirici, A. Thomas, M. Antonietti, *J. Mater. Chem.* **2007**, *17*, 3412 – 3418; f) S. Kubo, R. White, N. Yoshizawa, M. Antonietti, M. M. Titirici, *Chem. Mater.* **2011**, *23*, 4882 – 4885; g) H. Liang, Q. Guan, L. Chen, Z. Zhu, W. Zhang, S. H. Yu, *Angew. Chem.* **2012**, *124*, 5191 – 5195; *Angew. Chem. Int. Ed.* **2012**, *51*, 5101 – 5105; h) X. Cui, M. Antonietti, S. H. Yu, *Small* **2006**, *2*, 756 – 759; i) T. P. Fellinger, R. White, M. M. Titirici, M. Antonietti, *Adv. Funct. Mater.* **2012**, *22*, 3254 – 3260; j) R. White, N. Yoshizawa, M. Antonietti, M. M. Titirici, *Green Chem.* **2011**, *13*, 2428 – 2434; k) N. Baccile, M. Antonietti, M. M. Titirici, *ChemSusChem* **2010**, *3*, 246 – 253.

[5] a) J. Y. Yuan, M. Antonietti, *Polymer* **2011**, *52*, 1469 – 1482; b) Q. Zhao, P. F. Zhang, M. Antonietti, J. Y. Yuan, *J. Am. Chem. Soc.* **2012**, *134*, 11852 – 11855; c) J. Y. Yuan, S. Soll, M. Drechsler, A. H. E. Müller, M. Antonietti, *J. Am. Chem. Soc.* **2011**, *133*, 17556 – 17559.

[6] a) G. Hasegawa, K. Kanamori, K. Nakanishi, *Microporous Mesoporous Mater.* **2012**, *155*, 265 – 273; b) K. Kanamori, K. Nakanishi, *Chem. Soc. Rev.* **2011**, *40*, 754 – 770.

[7] a) Z. L. Xie, R. White, J. Weber, A. Taubert, M. Titirici, *J. Mater. Chem.* **2011**, *21*, 7434 – 7442; b) F. S. Asghari, H. Yoshida, *Ind. Eng. Chem. Res.* **2007**, *46*, 7703 – 7710.

[8] a) K. J. Klabunde, R. M. Richards, *Nanoscale Materials in Chemistry*, Wiley-VCH, Weinheim, **2009**; b) R. Petričević, G. Reichenauer, V. Bock, A. Emmerling, J. Fricke, *J. Non-Cryst. Solids* **1998**, *225*, 41 – 45.

[9] a) C. Chan-Thaw, A. Villa, G. Veith, K. Kailasam, L. Adamczyk, R. Unocic, L. Prati, A. Thomas, *Chem. Asian J.* **2012**, *7*, 387 – 393; b) G. Mane, S. Talapaneni, C. Anand, S. Varghese, H. Iwai, Q. Ji, K. Ariga, T. Mori, A. Vinu, *Adv. Funct. Mater.* **2012**, *22*, 3596 – 3604; c) K. K. R. Datta, B. V. S. Reddy, K. Ariga, A. Vinu, *Angew. Chem.* **2010**, *122*, 6097 – 6101; *Angew. Chem. Int. Ed.* **2010**, *49*, 5961 – 5965.

[10] a) H. Qian, M. Antonietti, S. H. Yu, *Adv. Funct. Mater.* **2007**, *17*, 637 – 643; b) Y. Lu, H. Zhu, W. Li, B. Hu, S. H. Yu, *J. Mater. Chem. A* **2013**, *1*, 3783 – 3788; c) B. Deng, A. Xu, G. Chen, R. Song, L. Chen, *J. Phys. Chem. B* **2006**, *110*, 11711 – 11716; d) J. Gong, S. H. Yu, H. Qian, L. Luo, T. Li, *J. Phys. Chem. C* **2007**, *111*, 2490 – 2496; e) W. Kang, H. Li, Y. Yan, P. Xiao, L. Zhu, K. Tang, Y. Zhu, Y. T. Qian, *J. Phys. Chem. C* **2011**, *115*, 6250 – 6256; f) H. Qian, S. H. Yu, L. Luo, J. Gong, L. Fei, X. Liu, *Chem. Mater.* **2006**, *18*, 2102 – 2108; g) X. Sun, Y. D. Li, *Angew. Chem.* **2004**, *116*, 607 – 611; *Angew. Chem. Int. Ed.* **2004**, *43*, 597 – 601.

[11] a) J. Li, Y. Zheng, J. Zeng, Y. Xia, *Chem. Eur. J.* **2012**, *18*, 8150 – 8156; b) D. Enache, J. Edwards, P. Landon, B. Solsona-Espriu, A. Carley, A. Herzing, M. Watanabe, C. Kiely, D. Knight, G. Hutchings, *Science* **2006**, *311*, 362 – 365; c) A. Henning, J. Watt, P. Miedziak, S. Cheong, M. Santonastaso, M. Song, Y. Takeda, A. Kirkland, S. Taylor, R. Tilley, *Angew. Chem.* **2013**, *125*, 1517 – 1520; *Angew. Chem. Int. Ed.* **2013**, *52*, 1477 – 1480.

[12] a) L. B. Belykh, T. V. Goremyka, L. N. Belonogova, F. K. Schmidt, *J. Mol. Catal. A* **2005**, *231*, 53 – 59; b) C. Li, Z. Shao, M. Pang, C. Williams, C. Liang, *Catal. Today* **2012**, *186*, 69 – 75.